NIH-PA Author Manuscript

NIH-PA Author Manuscript

NIH-PA Author Manuscript

The N-terminal half of the connexin protein contains the core elements of the pore and voltage gates

Jack Kronengold[1], **Miduturu Srinivas**[2], and **Vytas K. Verselis**[3]

[1]Department of Pharmacology, Yale University School of Medicine, New Haven, CT 06520

[2]Department of Biological Sciences, State University of New York College of Optometry, New York, NY 10036

[3]Dominick P. Purpura Department of Neuroscience, Albert Einstein College of Medicine, Bronx, NY

Abstract

Connexins form channels with large aqueous pores that mediate fluxes of inorganic ions and biological signaling molecules. Studies aimed at identifying the connexin pore now include a crystal structure that provides details of putative pore-lining residues that need to be verified using independent biophysical approaches. Here we extended our initial cysteine-scanning studies of the TM1/E1 region of Cx46 hemichannels to include TM2 and TM3 transmembrane segments. No evidence of reactivity was observed in either TM2 or TM3 probed with small or large thiol-modifying reagents. Several identified pore residues in E1 of Cx46 have been verified in different Cx isoforms. Use of variety of thiol reagents indicates that the connexin hemichannel pore is large and flexible enough, at least in the extracellular part of the pore funnel, to accommodate uncommonly large side chains. We also find that that gating characteristics are largely determined by the same domains that constitute the pore. These data indicate that biophysical and structural studies are converging towards a view that the N-terminal half of the Cx protein contains the principal components of the pore and gating elements, with NT, TM1 and E1 forming the pore funnel.

Keywords

channel pore; voltage gating connexin; cysteine scanning; chimera; hemichannels

Introduction

Connexins (Cxs) comprise a family of ion channels with large aqueous pores that can transmit a variety of biological signaling molecules including cyclic nucleotides, inositol 1,4,5-triphosphate (IP_3), ATP and, in some instances, small interfering RNAs (Evans et al., 2006; Harris, 2001; Neijssen et al., 2005; Valiunas et al., 2005). It is now evident that Cx channels function in two configurations, as gap junction (GJ) or cell-cell channels formed by the head-to-head docking of two hemichannels (connexons), and as undocked hemichannels. The latter function like conventional membrane ion channels in that they mediate transmission of signals across the plasma membrane, but the signals transmitted extend beyond small inorganic ions. Tissue-specific Cx expression (Willecke et al., 2002) and the

---
[*]To whom correspondence should be addressed. Dominick P. Purpura Department of Neuroscience, Albert Einstein College of Medicine, 1300 Morris Park Avenue, Bronx, New York 10461, Tel: 718-430-3680, Fax: 718-430-8944, vytas.verselis@einstein.yu.edu.

different reported selectivity profiles of Cxs (Goldberg et al., 2004; Harris, 2001; Veenstra et al., 1995; Verselis and Veenstra, 2000; Weber et al., 2004) suggest that that there are differences in the pores among Cx channels that can impact significantly on which signals are selected for transmission.

An interesting feature of Cx channels that originated from early studies in cell pairs is that GJ channels gate in response to the transjunctional voltage, V_j, the voltage difference between two cells, irrespective of the absolute membrane potentials that generate the V_j (Harris et al., 1981; Spray et al., 1981). This sensitivity suggests that the gating elements that sense voltage reside in the pore. Thus, differences in the pores among connexins that impact on selectivity may also impact on gating. Conserved gating characteristic of GJ channels and undocked hemichannels indicate that there is conservation of voltage gating structures in both Cx channel configurations (Bukauskas and Verselis, 2004; Verselis, 2009).

Recently, a crystal structure of a Cx26 GJ channel was obtained at 3.5 Å resolution and shows an overall pore structure that has wide entrances at the cytoplasmic ends of the two opposed hemichannels, narrowing to a funnel shape through the transmembrane spans and then widening slightly again in the extracellular region (Maeda et al., 2009). The topology of a connexin subunit consists of four membrane spanning segments, TM1 – TM4, with N-terminal (NT) and C-terminal (CT) domains located intracellularly and two extracellular loops, E1 and E2, connecting TM1 to TM2 and TM3 to TM4, respectively. In the crystal structure, the bulk of the putative pore proper, i.e. the so-called pore funnel, is formed by segments of NT, TM1 and E1 domains. The widest parts of the cytoplasmic entrances beyond the funnel are formed by parts of TM2 and TM3, which in Cx26 is rich in positively charged residues.

This assignment of NT, TM1 and E1 to the pore funnel essentially agrees with reports that preceded the crystal structure and deduced the pore configuration based on biophysical studies of gating in Cx32 and Cx26 GJ channels and substituted-cysteine accessibility studies in Cx46 and chimeric Cx32*43E1 hemichannels (Kronengold et al., 2003a; Oh et al., 2008; Purnick et al., 2000; Verselis, 2009; Verselis et al., 1994; Zhou et al., 1997). However, the charge selectivity of Cx26, which is biased towards cations, is not wholly compatible with the crystal structure and cysteine accessibility studies of Cx32 GJ channels using a cut-open oocyte preparation reported that some residues in TM1 and TM2 contributed to the cytoplasmic end of the pore with the channel in closed and open states, respectively (Skerrett et al., 2002). The same study reported TM3 as the major pore-lining helix throughout the transmembrane span.

Given these contrasting data and the need to test the general validity of the crystal structure as representative of a functional Cx channel, we applied the substituted cysteine accessibility method, SCAM, to the entire span of TM2 and TM3 in Cx46 hemichannels to extend published data in TM1 and E1 in the same connexin. In a subset of residues we also applied SCAM to Cx50 hemichannels, a connexin that despite close primary sequence homology with Cx46, exhibits a substantially larger unitary conductance and different voltage-dependent gating properties (Srinivas et al., 2005). We also examined unitary conductance and gating properties of a number of chimeric hemichannels composed of interchanged segments of Cx46 and Cx50 to determine whether gating and selectivity properties segregate together. We find that both the SCAM and chimeric data point to NT, TM1 and E1 domains as the core elements that constitute the connexin pore as well as the essential components necessary for voltage-dependent gating.

Materials and Methods

Construction of cysteine substitutions in TM2 and TM3

The rat Cx46 coding sequence was cloned into EcoRI-Hind III of pGem7*zf*(+) (Promega, Madison, WI) and was used as a template to construct the mutants. For construction of the TM2 Cys substitutions we introduced new restriction sites through silent mutagenesis (ApaI, PstI, SspI, SalI and AvrII) and created a new wtCx46 cassette called rCx46-M2mut. The PCR generated fragments containing the individual Cys mutations were subcloned as follows: EcoRI/SalI (F77C-Q81C), PstI (I82C-T87C), SalI/BssHII (P88C-L90C) and EcoRI/PmlI (I91C-G94C). To make TM3 mutants we first introduced SalI and MscI sites by silent mutagenesis into the full length wtCx46. A SalI/BstXI 330 bp fragment was cloned into pGem7*zf*(+) to make an rCx46-M3mut cassette which would allow for unique cloning sites. Mutants were generated on this cassette using PshAI/PstI (F157C-T163C), MscI/PmlI (L164C-I170C) and PstI/PmlI (A171C-F175C). Cysteine mutants were then backcloned into wtCx46. All constructs were sequenced over the restriction sites used for cloning.

Construction of chimeras composed of Cx46 and Cx50

The mouse Cx50 coding sequence was subcloned into the SP64T transcription vector (generously provided by Dr. Thomas White, SUNY, Stony Brook, NY). We constructed chimeras that exchanged Cx50 and Cx46 sequence. The chimeras are designated first by the parent Cx followed by the donor Cx and the sequence replaced by the donor Cx. Thus, Cx50*46NT-CL, has the N-terminal half of Cx50, NT through CL, replaced by Cx46 sequence. The chimeras were made using PshAI and BamHI as cloning sites for the respective gel purified inserts and vectors. The domains of the two connexins based on the alignment published in Bennett et al. (1991) are as follows: for Cx46, NT(Met1-Lys23), TM1 (Val24-Ala 41), E1(Glu42-Arg 76), TM2 (Phe77-Gly 94), CL (His 95 – Val 156), TM3 (Phe 157-Phe 175), E2 (Leu176-Thr207), TM4 (Ile 208 – Leu 226) and CT (Glu227-Ile 416). For Cx50, NT (Met 1 – Arg 23), TM1 (Val 24 – Ala 41), E1 (Glu 42 – Arg 76), TM2 (Leu 77 – Gly 94), CL (His 95 – Val 159), TM3 (Cys 160 – Phe 178), E2 (Leu 179 – Thr 210), TM4 (Ile 211 – Met 229), CT (Glu 230 – Ile 440). Both chimeras were sequenced over the sites used for cloning.

Expression of hemichannels in Xenopus oocytes

mRNA was prepared from appropriately linearized plasmid DNA with the mMessage mMachine T7 and SP6 RNA kits from Ambion (Austin, TX), according to the manufacturer's protocol. The mRNA was purified using QIAquick PCR purification columns from QIAGEN (Valencia, CA). mRNA bound to the column was eluted with 30–40 μl of an aqueous solution of DNA antisense to the endogenous *Xen*Cx38 (8 pmole/ml). We used the phosphorothioate antisense oligo 5'-GCT TTA GTA ATT CCC ATC CTG CCA TGT TTC-3', which is complementary to *Xen*Cx38 commencing at NT -5 with respect to the ATG initiation codon. Preparation of *Xenopus* oocytes has been described previously (Trexler et al., 2000). Each oocyte was injected with 50–100 nl of the mRNA/antisense solution. Injected oocytes were kept at 18°C in a standard ND96 solution containing (in mM) 88 NaCl, 1 KCl, 2 MgCl$_2$, 1.8 CaCl$_2$, 5 glucose, 5 HEPES, 5 pyruvate, pH adjusted to 7.6.

Preparation of reagents

The methane thiosulfonate (MTS) reagents 2-trimethylammonioethylmethane thiosulfonate (MTSET) and 2-sulfonatoethylmethane thiosulfonate (MTSES) were purchased from Anatrace (Maumee, Ohio). 2-biotinoylaminoethylmethane thiosulfonate (MTSEA biotin) and 2-(6-biotinoylaminohexanoyl-aminoethylmethane thiosulfonate (MTSEA biotin-X)

were purchased from Biotium (Hayward, CA). Aliquots of dry powder were prepared and stored in microcentrifuge tubes at −20°C. Prior to each experiment aliquots of MTSET or MTSES were dissolved in distilled water, chilled on ice, and in the case of MTSEA biotin and MTSEA biotin-X were dissolved in DMSO, to stock concentrations of 250 mM. Dilutions were made into IPS just prior to application to the desired final concentration (typically 0.5 to 1 mM). Activity of MTS reagents were periodically checked using a TNB assay (Karlin and Akabas, 1998).

Electrophysiological recording and analysis

Functional expression of Cys-substituted mutants was screened using two electrode voltage clamp recordings of macroscopic currents from single *Xenopus* oocytes using a GeneClamp 500 amplifier (Molecular Devices Corp, Sunnyvale CA). Oocytes were placed in ND96 solution and both current-passing and voltage-recording pipettes contained 1M KCl.

For patch clamp recordings of single hemichannel currents, *Xenopus* oocytes were manually devitellinized in a hypertonic solution consisting of (in mM) 220 Na aspartate, 10 KCl, 2 $MgCl_2$, 10 HEPES and then placed in the ND96 solution for recovery. Oocytes were then individually moved to a recording chamber, (RC-28, Warner Instruments Corp.) containing the patch pipette solution (IPS) which consisted of (in mM) 140 KCl, 1 $MgCl_2$, 5 HEPES, 1 $CaCl_2$, 3 EGTA, and pH adjusted to 8.0 with KOH. The bath compartment was connected via a 3M agar bridge to a ground compartment containing the same IPS solution. After excision of patches containing single hemichannels, instrumentation offsets were manually corrected in the absence of an applied voltage. Hemichannel activity at a fixed voltage was recorded to establish a baseline current after which the compartment was perfused with freshly prepared MTS reagent. Single hemichannel I–V curves were obtained before and after MTS application by applying 8 sec voltage ramps from −70 to +70 mV. Unitary conductances plotted represent the slope conductances at $V_m = 0$ obtained from fitted open channel I–V relations.

In all electrophysiological experiments, data was acquired with AT-MIO-16X D/A boards from National Instruments (Austin, TX) using our own acquisition software (developed by E.B. Trexler). For macroscopic currents, currents were acquired at 2 kHz and filtered at 500 Hz. For patch clamp experiments, currents were filtered at 1 kHz and data were acquired at 10 kHz.

Results

Single Channel SCAM of TM2 and TM3 with MTSET

Previously we showed that the extracellular end of TM1 extending into E1 contributes to the pore in Cx46 hemichannels (Kronengold et al., 2003b). Results of SCAM studies of substituted Cys mutants in TM2 of Cx46 hemichannels are shown in Fig. 1. We individually substituted 18 residues, F77 through G94, which according to the original accepted membrane topology encompasses TM2 (Bennett et al., 1991). Corresponding sequence of Cx26, for which the crystal structure was obtained, is shown along with the sequence of Cx50. Cysteine substitutions at three positions in Cx46 (P88, L90 and Y92) failed to produce functional hemichannel currents when expressed in *Xenopus* oocytes. Substitutions at three additional positions, I82, I83 and V85, resulted in poor expression, evidenced by consistently small macroscopic currents, such that single channel recordings could not be reliably obtained. At the remaining positions, cysteine substitutions produced hemichannels with near wild-type unitary conductance values. At each of these positions, application of MTSET to the bath and subsequent patching did not show any substantial changes in unitary conductance (Fig. 1) or in open hemichannel rectification (data not shown).

In the same way, we applied SCAM to the entire putative TM3 domain, which included residues F157 through F175 (Fig. 2). Cys substitutions were generally well-tolerated throughout TM3 with Cys-substitutions at two positions (F165C and T163C) failing to produce functional hemichannels. As for TM2, application of MTSET did not show any substantial changes in single hemichannel properties at any of the positions. Data for the extracellular half, E166 to F175, probed with MTSET applied to extracellular and intracellular sides in excised patches was previously reported and showed no evidence of reactivity (Kronengold et al., 2003a; Kronengold et al., 2003b).

SCAM using a large MTS reagent, MTSEA biotin-X

Assignment of TM3 to the pore in studies of Cx32 gap junction channels used, maleimidobutyrylbiocytin (MBB) as the thiol reagent and use of a smaller thiol reagent could potentially fail to produce significant changes in unitary conductance in a large channel. Thus, we re-examined a subset of residues in TM3 at the single hemichannel level using a large MTS reagent, MTSEA biotin-X (MW=485). Fig. 3 shows an alignment of TM3 residues in Cx32, Cx46 and Cx50. Arrows indicate the 7 positions reported to be reactive in Cx32 GJs (Skerrett et al., 2002). We examined the corresponding positions in Cx46 hemichannels (boxed) using MTSEA biotin-X are Y155, I159, F161, L164, V167, F169 and A171 in Cx46. We also examined 3 corresponding positions in Cx50, Y158, V170 and F172 (boxed). No substantial changes in unitary conductance upon application of this reagent were found at any of the TM3 positions in Cx46 or Cx50 hemichannels, consistent with results obtained with MTSET. In contrast, results using a large MTSEA biotin-X reagent with a cysteine substituted at identified pore-lining positions showed large effects on conductance that differed from those observed using MTSET. In the example shown in Fig. 4, application of MTSEA biotin-X to an excised patch containing an F43C substitution at the TM1/E1 border of Cx50 resulted in a step-wise reduction in current that did not reverse upon wash-out of the reagent, indicative of covalent modification. The step-wise reduction in current occurred within seconds of application resulting in a final single channel current that was reduced by >90% and displayed a very noisy, flickery behavior. Often 5 or 6 steps were discernible consistent with modification of most or all Cx subunits. In this example, 5 steps were visible and are illustrated at a higher time resolution below. These results indicate that the hemichannel pore is large enough and/or flexible enough to potentially accommodate all six biotin-X side chains. A bar graph showing the reductions in unitary current for four MTS reagents, MTSET and MTSES that differ in charge, and MTSEA biotin and MTSEA biotin-X that are large in size (Fig. 4B). The results show a large reduction for MTSET compared to MTSES and even larger reductions for the MTSEA biotin and MTSEA biotin–X reagents consistent with both electrostatic and steric effects on ion conduction. Moreover, the same results as shown in Fig. 4 could be obtained with reagent added from either extracellular or cytoplasmic sides of the hemichannel demonstrating that this large reagent is readily permeable.

Molecular determinants of single hemichannel conductance and gating reside within the N-terminal half

To assess what parts of the connexin protein are important for determining Cx-specific conductance and gating properties, we utilized Cx46 and Cx50, which possess a high degree of sequence homology (White et al., 1992) yet exhibit substantially different unitary conductances and voltage gating characteristics (Srinivas et al., 2005). Unitary conductance measured as the slope conductance at $V_m=0$ in 140mM symmetric KCl was ~290 pS for Cx46 and ~470 pS for Cx50. As far as gating, closure at negative voltages, which is mediated by one of two intrinsic mechanisms termed loop or slow gating (Bukauskas and Verselis, 2004; Trexler et al., 1996), is poorly sensitive to voltage in Cx50 when extracellular Ca^{2+} is chelated to sub-micromolar levels with EGTA and Mg^{2+} and

maintained at physiological (1 – 2 mM) concentrations. Conversely, Cx46 hemichannels under these same conditions close steeply with voltages between −50 and −90 mV (Srinivas et al., 2005). Closure at positive voltages, mediated by another mechanism termed V_j or fast gating (Bukauskas and Verselis, 2004) is similar in both connexins, albeit somewhat more sensitive in Cx50.

We constructed chimeras to exchange domains between Cx46 and Cx50 and examined the accompanying changes in unitary conductance and gating. Data are summarized in Figs. 5 and 6. For the most part, substitution of the N-terminal half (NT-CL) of Cx46 with Cx50 sequence (Cx46*50NT-CL) and the reciprocal chimera, Cx50*46NT-CL, produced hemichannels that were indistinguishable from the donor Cxs, in terms of unitary conductance (Fig. 5). Open hemichannel rectification was also the same (not shown). Substitution of just the N-terminal domain, to yield Cx46*50NT and Cx50*46NT chimeras (arrows), resulted in functional hemichannels with unitary conductances that were remarkably altered and closer in value to the respective donor Cxs (Fig. 5). Cx50*46NT-E1 and Cx50*46NT-TM2 were also similar to the donor Cx46. Thus, the NT, TM1 and E1 domains appear to be sufficient to specify unitary conductance and in the case of Cx46 sequence onto Cx50, and NT appears to be most responsible for the differences in their conductances. Unfortunately, the reciprocal chimeras, Cx46*50NT-E1 and Cx46*50NT-TM2 lacked function.

For gating, substitution of NT of Cx50 with Cx46 (Cx50*46NT) had little impact on loop gating, whereas the reciprocal chimera, Cx46*50NT, had a large impact (Fig. 6). The latter, however, appeared to open with hyperpolarizing voltages, unlike WT Cx50. The Cx50*46NTE1 and Cx50*46NT-TM2 dramatically changed loop gating and actually made it more sensitive to voltage with faster kinetics of closure than the WT Cx46. Finally, the reciprocal Cx46*50NTCL and Cx50*46NT-CL chimeras, that exchanged domains NT through CL recapitulated the gating characteristics of the donor Cxs, Cx50 and Cx46 respectively. Thus, in order to fully reconstruct gating, sequence extending from NT and into the CL domain had to be included.

Discussion

There is now corroborating structural and electrophysiological evidence that the bulk of the connexin pore is formed by NT, TM1 and E1 domains. Our original SCAM study in Cx46 focused on TM1 and E1 domains and showed large effects on unitary conductance upon modification with MTS reagents (Kronengold et al., 2003b). Moreover, the effects differed upon modification with the positively and negatively charged MTS regents, MTSET and MTSES, respectively, consistent with the expected electrostatic effects on ion transport in a pore that better selects for cations over anions.

Here we applied SCAM to TM2 and TM3 domains of Cx46 hemichannels and extended the study to larger MTS reagents as well as to another Cx. Given the SCAM study on Cx32 that reported TM3 in GJs to be pore-lining using MBB, a large thiol reagent (Skerrett et al., 2002), we applied SCAM to hemichannels using a large MTS reagent with the idea that use of only smaller reagents could produce minimal effects, particularly at wider regions of the Cx pore. Using the criteria that modification must affect unitary conductance and occur with reagent added to either side of the membrane, we did not see evidence of accessibility in any of the residues in TM2 (F77 – G94) or TM3 (F157 – F175). Moreover, the subset of residues reported as pore-lining in TM3 of Cx32 GJs showed no reactivity in Cx46 when probed with the larger MTS biotin-X reagent. Several residues probed in Cx50 as well, showed no reactivity. In this study, we only screened TM2 and TM3 from the outside, i.e. we applied MTS reagents to extracellular side, but the lack of any effect fulfills the criteria for

exclusion from the pore. These data indicate that either there is no exposure of TM2 and TM3 domains to the pore of open Cx46 hemichannels or that modifications are occurring, even with large thiol reagents, but that they constitute silent modifications. We reason that silent modifications are unlikely to occur if a residue is in the conducting pathway because placing 6 charges, even in a wide region, should alter the concentration of mobile counterions thereby affecting unitary conductance and rectification. Also, placing sufficient bulk that nearly occludes the hemichannel pore in the narrower regions, i.e. MTSEA biotin-X, would likely have some impact on conductance, at least in the form of open hemichannel noise. However, we cannot definitively rule out that silent modifications can occur. We did not check for effects on gating, which could produce changes in macroscopic currents as a result of changes in open probability irrespective of whether or not a residue resides in the pore.

An interesting observation is that most positions in TM2 and TM3 were remarkably well tolerated by Cys substitutions with no perceptible changes in open hemichannel properties. Only a handful of Cys substitutions within these TM domains showed loss of function, which included P88C, L90C and Y92C in TM2 and T163C and F165C in TM3. P88 and nearby positions in TM2 have been shown to be important in gating via a proline-kink motif (Ri et al., 1999) and may disrupt channel function. It is unclear why T163 and F165 failed to function as hemichannels and we did not examine how these substitutions affected GJ channel function. Failure of both would suggest a more general disruption of structure, whether through changes helical structure and/or contacts with other helices. I82C and I83C in TM2 were functional, but displayed altered gating. With the exception of P88, none of these positions are associated with mutations that cause cataractogenesis.

Pore residues identified in E1 of Cx46 include E43, G46 and D51. These same residues are also reacted in SCAM studies of Cx50 (Verselis et al., 2009), although, perhaps, not surprising given the high degree of homology between Cx46 and Cx50. However, we recently demonstrated that the one of these homologous positions in Cx26, G45, is pore-lining (Sanchez et al., 2010) and the G45E mutation leads to a severe form of syndromic deafness (Janecke et al., 2005; Lee et al., 2009). Thus, there appears to be correspondence among distantly related Cxs, as well, an indication that overall pore structure may be conserved among all Cxs, although more members of the Cx family need to be examined. Systematic comparison of differences among all pore-lining residues, once identified, could provide a basis for Cx-specific differences in conductance and selectivity. However, the principal domains contributing to the pore, although conserved among Cxs, can undergo small perturbations in structure that can impart shifts in the positions of specific residues within pore-lining segments. Complicating this view is the possibility that post-translational modifications of key residues can modulate properties independent of whether coded sequence is conserved (Kwon et al., 2011; Locke et al., 2009).

At identified pore lining positions in Cx46 and Cx50, such E(F)43 or G46, modifications with different MTS reagents produce different effects on open hemichannel properties consistent with a strong impact of charge as well as size. The side chain that results from modification by MTSES is bulkier that that with MTSET, yet MTSES typically produced a small increase in unitary conductance. Thus, there is a considerable electrostatic effect on ion flux in this region of the pore. Introduction of a positive charge at one pore-lining position can reduce conductance substantially and in the case of Cx50, modification of F43 to a positive charge reduced conductance by ~70%. These electrostatic effects are consistent with a pore that is biased with negative charge, giving rise to a preferential flux of cations. Indeed, Cx46 and Cx50 have been shown to prefer cations over anions (Srinivas et al., 1999; Trexler et al., 1996; Trexler et al., 2000). Modification of F43 with larger reagents, MTS biotin and MTS biotin-X produced even larger reductions in unitary conductance consistent

with steric impedance to ion flux. The reductions were accompanied by large, noisy fluctuations, not resolvable by the patch clamp amplifiers that likely represent atomic motions of the biotin moieties. Perhaps surprising was that these large reagents produced 5 or 6 step-reductions in current consistent with modification of most or all six subunits. This result indicates that the F43 position, which is within the pore funnel identified by the Cx26 structure, allows sequential access of six MTS biotin-X molecules leading to six modified side chains. Thus, the pore must be quite wide and/or show enough flexibility to accommodate six large side chains. It will be interesting to determine whether other positions accommodate less molecules or show different degrees of noise, perhaps indicative of narrowed diameter and/or increased rigidity.

A potential link between selectivity and gating comes from the positioning of Cx voltage sensors within the pore. This arrangement comes from studies demonstrating sensitivity of GJ channels to V_j, irrespective of the absolute membrane potentials of the coupled cells (Harris et al., 1981; Spray et al., 1981). This arrangement applies to both intrinsic voltage gating mechanisms, loop or slow gating and V_j or fast gating (Bukauskas and Verselis, 2004). In the absence of docking, the same sensors now respond to the membrane potential as the reference potential of the coupled cell is replaced by the extracellular milieu.

Knowing more about the pore structure, we examined chimeras that exchanged domains between Cx46 and Cx50, which exhibit substantially different loop gating characteristics and unitary conductances (Srinivas et al., 2005) despite close sequence homology. Reciprocally substituting just the NT domain had a huge impact on unitary conductance and rather than resulting in intermediate conductances, the Cx50*46NT and Cx46*50NT chimeras produced somewhat smaller and larger unitary conductances, respectively than the corresponding donor Cxs. Effects on loop gating were widely disparate, with minimal changes occurring when substituting NT of Cx46 on Cx50 (Cx50*46NT), but loss of the characteristically strong closure of the loop gate of Cx46 when substituting NT of Cx50 onto Cx46 (Cx46*50NT). Inclusion of more domains of Cx46 onto Cx50, *46NT-E1 and *46NT-TM2, remarkably converted the weak loop gating of Cx50 into one that resembled Cx46, except that closure was even more robust and displayed faster kinetics. Surprisingly, reciprocal chimeras were not functional. However, consistent with SCAM studies, the unitary hemichannel properties acquired all of the characteristics of the donor Cxs when the N-terminal half (NT through CL) was substituted. Likewise, gating characteristics were also transferred. These data are consistent with mutational studies on chick homologs of Cx46 and Cx50 (Tong and Ebihara, 2006; Tong et al., 2004) as well as chimeric studies that exchanged domains between Cx32 and Cx37 (Hu et al., 2006). Cx43 differs in that truncation of CT or tagging it with EGFP results in loss of V_j gating (Bukauskas et al., 2001; Moreno et al., 2002). NMR studies have shown that CT interacts with CL (Duffy et al., 2002), which may, in turn, interact with NT thereby affecting V_j gating. This property may be unique to Cx43 as tagging or truncating CT in other Cxs does not appear to affect gating.

Taken together, these data suggest that gating and conductance co-segregate, but that the relationship is, not surprisingly, complex. The disparate effects on loop gating upon substitution of NT alone indicate that there is likely an intimate association of NT with other parts of protein, which in the case of Cx46 and Cx50 appears to occur within TM1 through E1. This observation is in support of the crystal structure that suggests there are interactions between NT and TM1 that keep the NT domain up against the channel wall, thereby keeping the pore unobstructed. It remains to be determined whether this specific interaction mediates gating. The lack of function for chimeras that substitute NT-E1 and NT-TM2 sequence of Cx50 onto Cx46 suggest that the putative interactions between NT and TM1 are very sensitive to structural perturbations, and may require inclusion of NT through CL. Although TM3, E2, TM4 and CT sequences may not contain the core elements that determine

differences in conductance and gating properties among Cxs, helix packing can undoubtedly be disrupted with substitutions in these regions resulting in effects on channel properties. However, these will often lead to loss of function or effects that are not consistent among members of the Cx family.

In conclusion, biophysical and structural studies are converging towards a view that the Cx pore is principally formed by NT, TM1 and E1 domains and that this structure is conserved among all members of the Cx family. An additional contribution to the pore suggested by the crystal structure includes a region of positive charge in the CL region (now assigned as an extension of the TM2 helix) that resides at the cytoplasmic entrance. These charges are incompatible with the selectivity characteristics of Cx26 and an equilibrated structure of Cx26 resulting from molecular dynamics simulations suggest that neutralization of these charges is required to produce cation flux through the channel (Kwon et al., 2011). Moving forward, there is now a framework within which to continue testing and refining models of gating and permeability as functional studies test structural motifs and identified interactions. Agreement between structure and function will come by continued biophysical studies concomitant with higher resolution structures crystallized in various states.

Acknowledgments

References

Bennett MV, Barrio LC, Bargiello TA, Spray DC, Hertzberg E, Saez JC. Gap junctions: new tools, new answers, new questions. Neuron. 1991; 6:305–320. [PubMed: 1848077]

Bukauskas FF, Bukauskiene A, Bennett MV, Verselis VK. Gating properties of gap junction channels assembled from connexin43 and connexin43 fused with green fluorescent protein. Biophys J. 2001; 81:137–152. [PubMed: 11423402]

Bukauskas FF, Verselis VK. Gap junction channel gating. Biochim Biophys Acta. 2004; 1662:42–60. [PubMed: 15033578]

Duffy HS, Delmar M, Spray DC. Formation of the gap junction nexus: binding partners for connexins. J Physiol Paris. 2002; 96:243–249. [PubMed: 12445902]

Evans WH, De Vuyst E, Leybaert L. The gap junction cellular internet: connexin hemichannels enter the signalling limelight. Biochem J. 2006; 397:1–14. [PubMed: 16761954]

Goldberg GS, Valiunas V, Brink PR. Selective permeability of gap junction channels. Biochim Biophys Acta. 2004; 1662:96–101. [PubMed: 15033581]

Harris AL. Emerging issues of connexin channels: biophysics fills the gap. Q Rev Biophys. 2001; 34:325–472. [PubMed: 11838236]

Harris AL, Spray DC, Bennett MV. Kinetic properties of a voltage-dependent junctional conductance. J. Gen. Physiol. 1981; 77:95–117. [PubMed: 6259275]

Hu X, Ma M, Dahl G. Conductance of connexin hemichannels segregates with the first transmembrane segment. Biophys J. 2006; 90:140–150. [PubMed: 16214855]

Janecke AR, Hennies HC, Gunther B, Gansl G, Smolle J, Messmer EM, Utermann G, Rittinger O. GJB2 mutations in keratitis-ichthyosis-deafness syndrome including its fatal form. Am J Med Genet A. 2005; 133:128–131. [PubMed: 15633193]

Karlin A, Akabas MH. Substituted-cysteine accessibility method. Methods Enzymol. 1998; 293:123–145. [PubMed: 9711606]

Kronengold J, Trexler EB, Bukauskas FF, Bargiello TA, Verselis VK. Porelining residues identified by single channel SCAM studies in Cx46 hemichannels. Cell Commun Adhes. 2003a; 10:193–199. [PubMed: 14681015]

Kronengold J, Trexler EB, Bukauskas FF, Bargiello TA, Verselis VK. Single-channel SCAM identifies pore-lining residues in the first extracellular loop and first transmembrane domains of Cx46 hemichannels. J Gen Physiol. 2003b; 122:389–405. [PubMed: 12975451]

Kwon T, Harris AL, Rossi A, Bargiello TA. Molecular dynamics simulations of the Cx26 hemichannel: evaluation of structural models with Brownian dynamics. J Gen Physiol. 2011; 138:475–493. [PubMed: 22006989]

Lee JR, Derosa AM, White TW. Connexin mutations causing skin disease and deafness increase hemichannel activity and cell death when expressed in Xenopus oocytes. J Invest Dermatol. 2009; 129:870–878. [PubMed: 18987669]

Locke D, Bian S, Li H, Harris AL. Post-translational modifications of connexin26 revealed by mass spectrometry. Biochem J. 2009; 424:385–398. [PubMed: 19775242]

Maeda S, Nakagawa S, Suga M, Yamashita E, Oshima A, Fujiyoshi Y, Tsukihara T. Structure of the connexin 26 gap junction channel at 3.5 A resolution. Nature. 2009; 458:597–602. [PubMed: 19340074]

Moreno AP, Chanson M, Elenes S, Anumonwo J, Scerri I, Gu H, Taffet SM, Delmar M. Role of the carboxyl terminal of connexin43 in transjunctional fast voltage gating. Circ Res. 2002; 90:450–457. [PubMed: 11884375]

Neijssen J, Herberts C, Drijfhout JW, Reits E, Janssen L, Neefjes J. Cross-presentation by intercellular peptide transfer through gap junctions. Nature. 2005; 434:83–88. [PubMed: 15744304]

Oh S, Verselis VK, Bargiello TA. Charges dispersed over the permeation pathway determine the charge selectivity and conductance of a Cx32 chimeric hemichannel. J Physiol. 2008; 586:2445–2461. [PubMed: 18372303]

Purnick PE, Oh S, Abrams CK, Verselis VK, Bargiello TA. Reversal of the gating polarity of gap junctions by negative charge substitutions in the N-terminus of connexin 32. Biophys. J. 2000; 79:2403–2415. [PubMed: 11053119]

Ri Y, Ballesteros JA, Abrams CK, Oh S, Verselis VK, Weinstein H, Bargiello TA. The role of a conserved proline residue in mediating conformational changes associated with voltage gating of Cx32 gap junctions. Biophys. J. 1999; 76:2887–2898. [PubMed: 10354417]

Sanchez HA, Mese G, Srinivas M, White TW, Verselis VK. Differentially altered Ca2+ regulation and Ca2+ permeability in Cx26 hemichannels formed by the A40V and G45E mutations that cause keratitis ichthyosis deafness syndrome. J Gen Physiol. 2010; 136:47–62. [PubMed: 20584891]

Skerrett IM, Aronowitz J, Shin JH, Cymes G, Kasperek E, Cao FL, Nicholson BJ. Identification of amino acid residues lining the pore of a gap junction channel. J Cell Biol. 2002; 159:349–360. [PubMed: 12403817]

Spray DC, Harris AL, Bennett MV. Equilibrium properties of a voltage-dependent junctional conductance. J. Gen. Physiol. 1981; 77:77–93. [PubMed: 6259274]

Srinivas M, Costa M, Gao Y, Fort A, Fishman GI, Spray DC. Voltage dependence of macroscopic and unitary currents of gap junction channels formed by mouse connexin50 expressed in rat neuroblastoma cells. J. Physiol. (Lond). 1999; 517:673–689. [PubMed: 10358109]

Srinivas M, Kronengold J, Bukauskas FF, Bargiello TA, Verselis VK. Correlative studies of gating in Cx46 and Cx50 hemichannels and gap junction channels. Biophys J. 2005; 88:1725–1739. [PubMed: 15596513]

Tong JJ, Ebihara L. Structural determinants for the differences in voltage gating of chicken Cx56 and Cx45.6 gap-junctional hemichannels. Biophys J. 2006; 91:2142–2154. [PubMed: 16798801]

Tong JJ, Liu X, Dong L, Ebihara L. Exchange of gating properties between rat cx46 and chicken cx45.6. Biophys J. 2004; 87:2397–2406. [PubMed: 15454438]

Trexler EB, Bennett MV, Bargiello TA, Verselis VK. Voltage gating and permeation in a gap junction hemichannel. Proc. Natl. Acad. Sci. U S A. 1996; 93:5836–5841. [PubMed: 8650179]

Trexler EB, Bukauskas FF, Kronengold J, Bargiello TA, Verselis VK. The first extracellular loop domain is a major determinant of charge selectivity in connexin46 channels. Biophys. J. 2000; 79:3036–3051. [PubMed: 11106610]

Valiunas V, Polosina YY, Miller H, Potapova IA, Valiuniene L, Doronin S, Mathias RT, Robinson RB, Rosen MR, Cohen IS, Brink PR. Connexin-specific cell-to-cell transfer of short interfering RNA by gap junctions. J Physiol. 2005; 568:459–468. [PubMed: 16037090]

Veenstra RD, Wang HZ, Beblo DA, Chilton MG, Harris AL, Beyer EC, Brink PR. Selectivity of connexin-specific gap junctions does not correlate with channel conductance. Circ. Res. 1995; 77:1156–1165. [PubMed: 7586229]

Verselis, VK. The Connexin Chanel Pore:Pore-lining Segments and Residues. In: Harris, D, ALaL, editor. Connexins:A Guide. New York, N.Y.: Humana Press; 2009. p. 77-102.

Verselis VK, Ginter CS, Bargiello TA. Opposite voltage gating polarities of two closely related connexins. Nature. 1994; 368:348–351. [PubMed: 8127371]

Verselis VK, Trelles MP, Rubinos C, Bargiello TA, Srinivas M. Loop gating of connexin hemichannels involves movement of pore-lining residues in the first extracellular loop domain. J Biol Chem. 2009; 284:4484–4493. [PubMed: 19074140]

Verselis, VK.; Veenstra, R. Gap junction channels Permeability and voltage gating Advances in Molecular and Cell Biology. In: Hertzberg, EL., editor. Gap Junctions. Elsevier; 2000. p. 129-192.

Weber PA, Chang HC, Spaeth KE, Nitsche JM, Nicholson BJ. The permeability of gap junction channels to probes of different size is dependent on connexin composition and permeant-pore affinities. Biophys J. 2004; 87:958–973. [PubMed: 15298902]

White TW, Bruzzone R, Goodenough DA, Paul DL. Mouse Cx50, a functional member of the connexin family of gap junction proteins, is the lens fiber protein MP70. Mol. Biol. Cell. 1992; 3:711–720. [PubMed: 1325220]

Willecke K, Eiberger J, Degen J, Eckardt D, Romualdi A, Guldenagel M, Deutsch U, Sohl G. Structural and functional diversity of connexin genes in the mouse and human genome. Biol Chem. 2002; 383:725–737. [PubMed: 12108537]

Zhou XW, Pfahnl A, Werner R, Hudder A, Llanes A, Luebke A, Dahl G. Identification of a pore lining segment in gap junction hemichannels. Biophys. J. 1997; 72:1946–1953. [PubMed: 9129799]
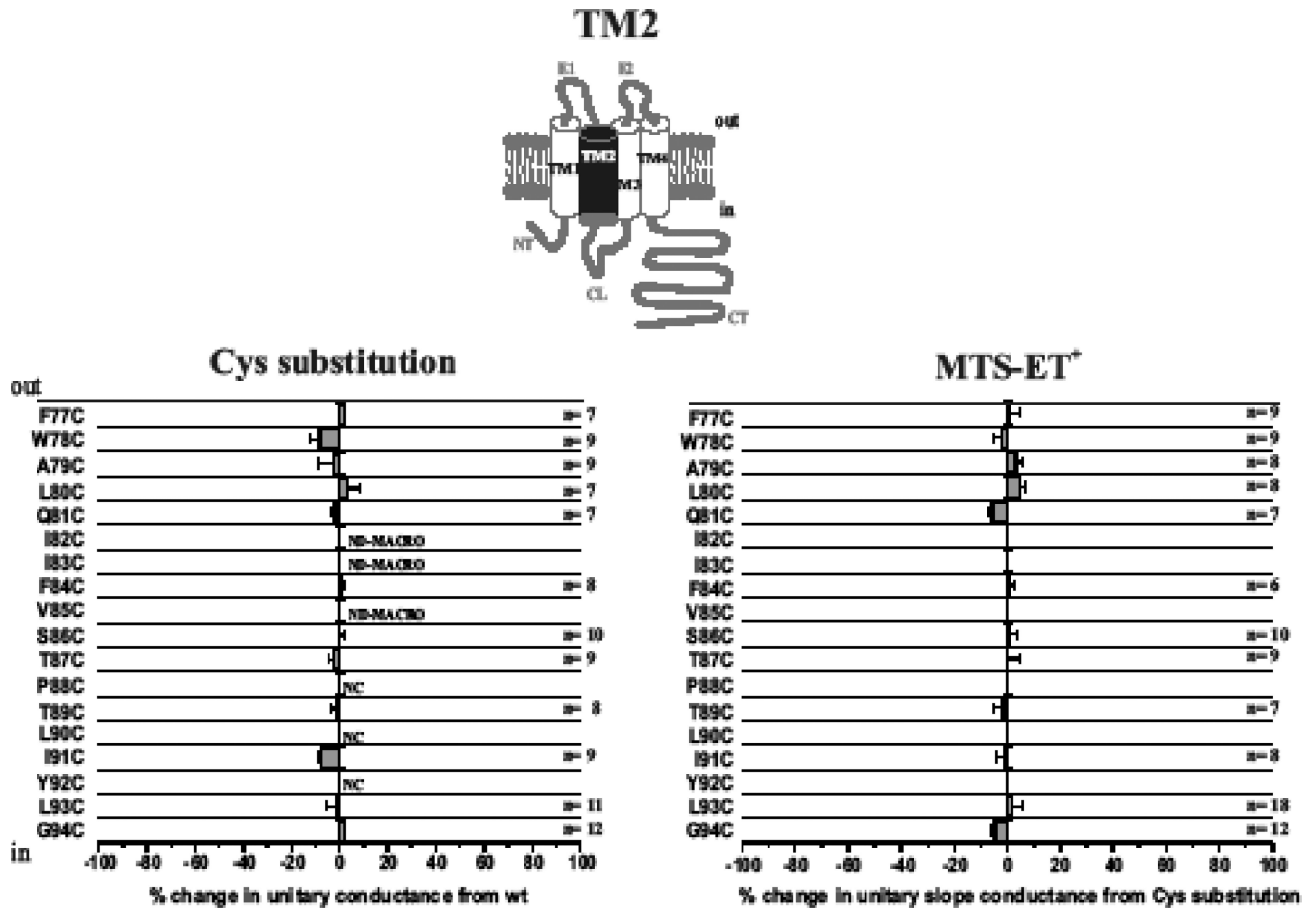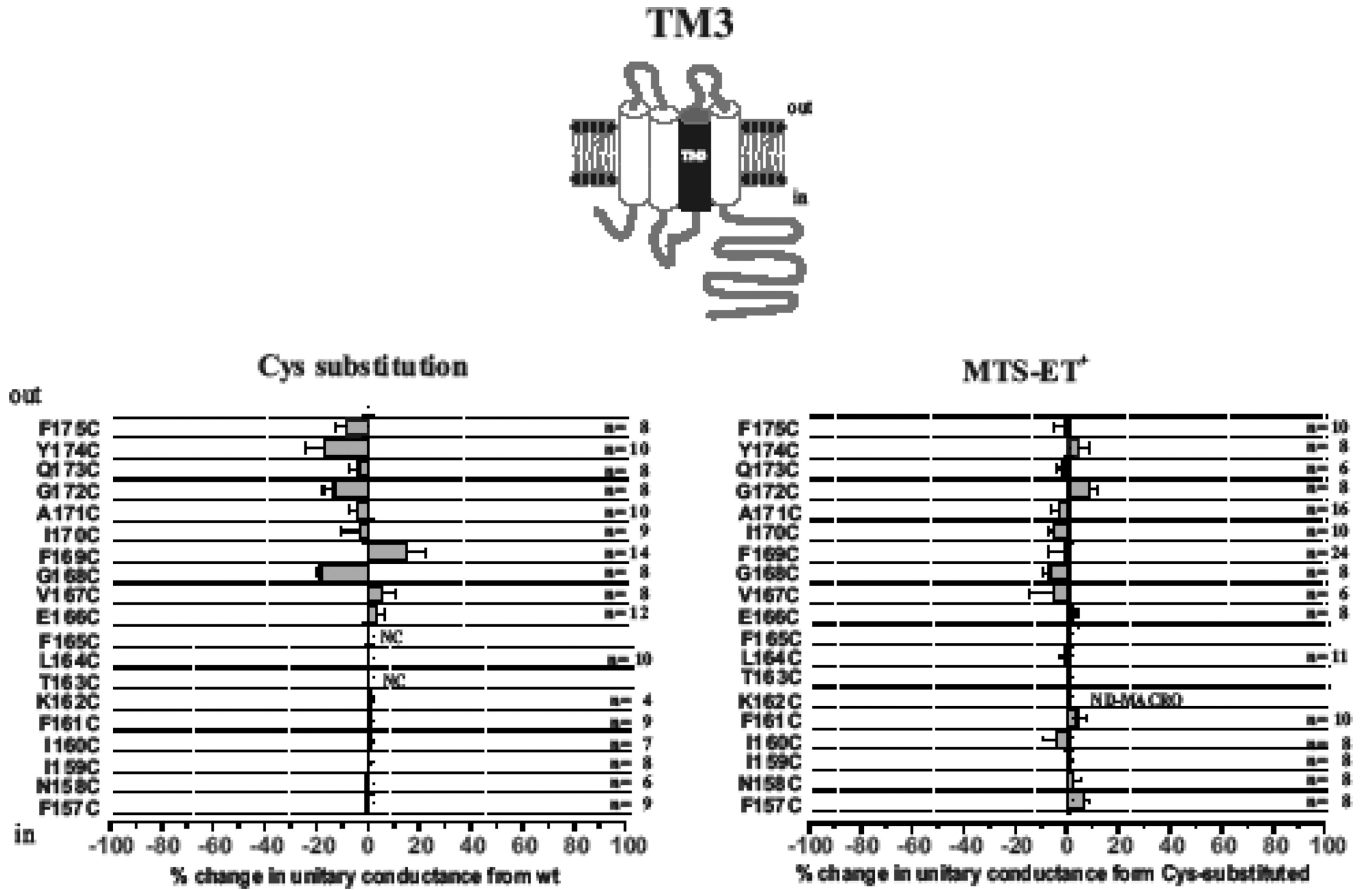
Fig. 1.
TM2 does not contribute to the pore in open Cx46 hemichannels. Shown are effects of Cys substitutions for TM2 residues F77 through G94 (left) and SCAM results using MTSET (right). For the Cys substitutions, the change in unitary conductance represents the mean percentage change in the slope conductance compared with wt Cx46 measured at $V_m = 0$ from fitted open channel I–V relations. Of the 18 residues examined, only P88C, L90C and Y92C failed to form functional hemichannels. In addition, single hemichannels were not observed from oocytes injected with I82C and V85C due to consistently low expression levels. For the SCAM results, the change in unitary conductance represents the mean percentage change in the slope conductance relative to the Cys substituted mutant measured at $V_m = 0$ from fitted open channel I–V relations. No substantial changes were observed at any positions. NC denotes nonfunctional hemichannels. ND-MACRO denotes residues for which there was insufficient single-channel data for characterization but macroscopic data in ND96 with 2mM Ca^{2+} and 0.2mM Ca^{2+} showed no reactivity. Error bars represent standard deviations; n 8 for each mutant.

Fig. 2.
TM3 does not contribute to the pore in open Cx46 hemichannels. Shown are effects of Cys substitutions for TM3 residues F157 through F175 (left) and SCAM results using MTSET (right). For the Cys substitutions, the change in unitary conductance represents the mean percentage change in the slope conductance compared with wt Cx46 measured at $V_m = 0$ from fitted open channel I–V relations. Of the 19 residues examined, only F163CF failed to form functional hemichannels and single hemichannels were not observed from oocytes injected with K162C due to consistently low expression levels. For the SCAM results, the change in unitary conductance represents the mean percentage change in the slope conductance relative to the Cys substituted mutant measured at $V_m = 0$ from fitted open channel I–V relations. No substantial changes were observed at any positions. NC denotes nonfunctional hemichannels. ND-MACRO denotes residues for which there was insufficient single-channel data for characterization but macroscopic data in ND96 with 2mM Ca^{2+} and 0.2mM Ca^{2+} showed no reactivity. Error bars represent standard deviations; n 8 for each mutant.
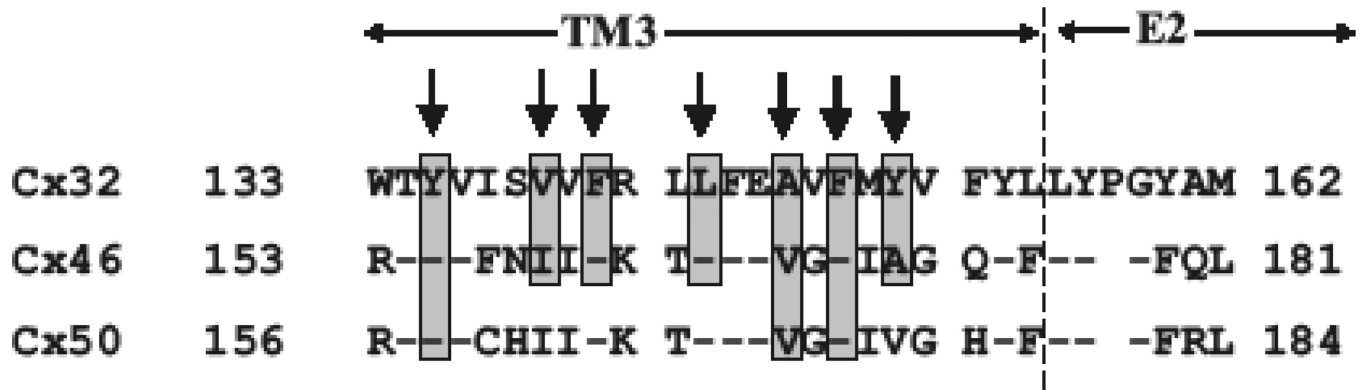
Fig. 3.
SCAM of select TM3 residues using a large MTS reagent shows no evidence of reactivity.
Shown is an alignment of Cx32, Cx46 and Cx50 sequence from the CL/TM3 border through
the proximal portion of E2. Residues indicated by arrows in Cx32 were reported to be pore-
lining in Cx32 GJ channels (Skerrett et al., 2002). Boxed residues in Cx46 and Cx50 were
subjected to SCAM analysis using MTS biotin-X. These include Y155, I159, F161, V167,
F169 and A171 in Cx46 and Y158, V170 and F172 in Cx50. No effects were observed at
any of these positions.

Cx50(F43C)
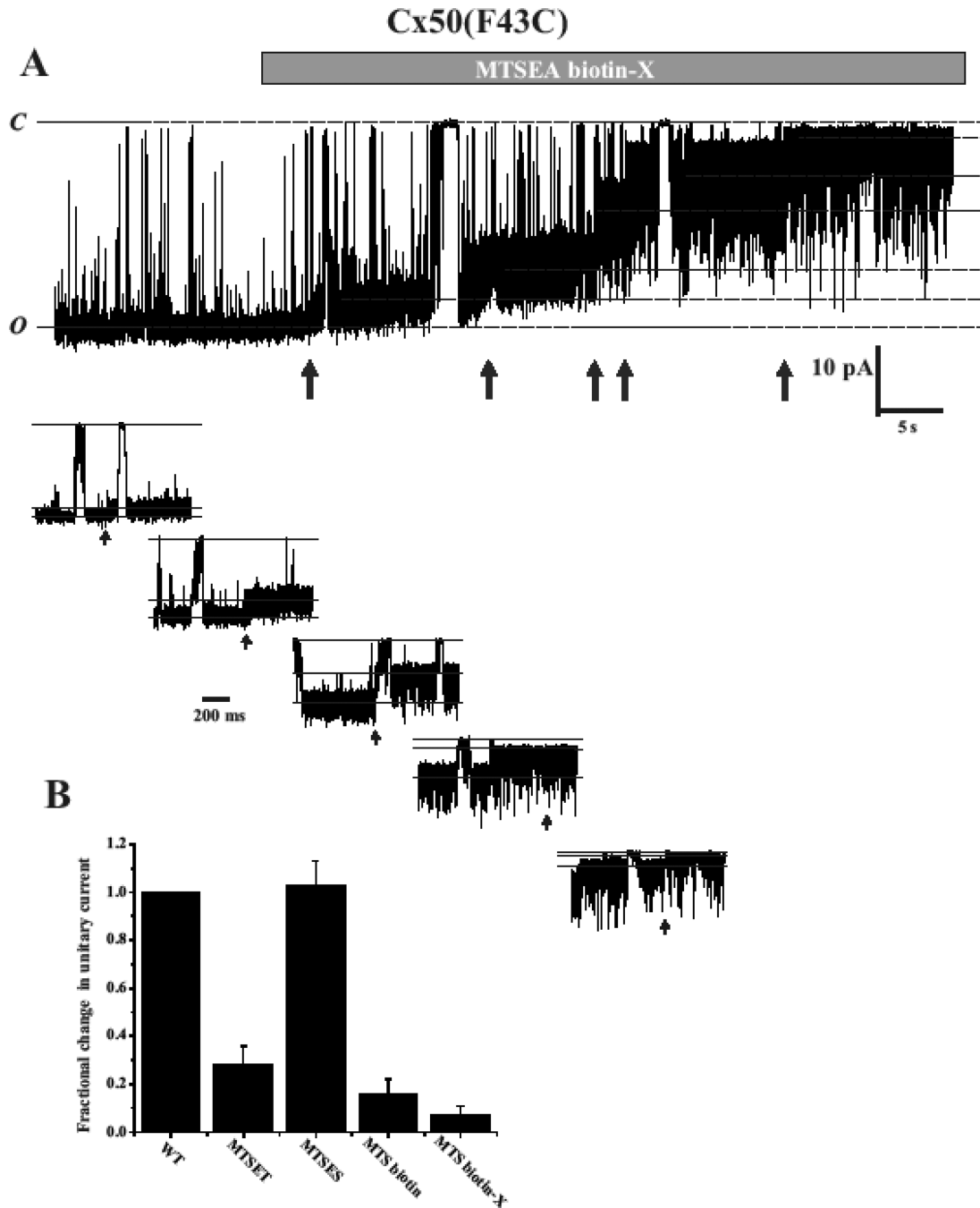
Fig. 4.
Multiple subunits in a Cx pore are modified by large MTS reagents. (A) Example of MTSEA-biotin-X modification of a single F43C hemichannel recorded in the outside-out patch configuration. The membrane potential was held at −50 mV. Application of MTSEA biotin-X (100 μM) caused a stepwise reduction in the single hemichannel current (arrows). The final conductance is markedly reduced and shows substantial flicker. At least five distinct changes in current were observed indicating modification of individual cysteines. Each of the modifications is shown in an expanded time scale. The step changes in current are rapid, consistent with chemical modification and the hemichannel continues to gate even with multiple subunits modified. The degree of flicker increases with the number of

modified subunits. (B) Bar graph summarizing reductions in current for in Cx50(F43C) hemichannels after modification with different MTS reagents. Currents were observed at a holding current of −40 or −50 mV and are expressed as fractional currents remaining relative to those before reaction. The data represent reductions of 72% (n=8), 84% (n=5) and 93% (n=5) for MTSET, MTSEA-biotin and MTSEA-biotin-X, respectively and a small increase (5%, n=4) for MTSES.
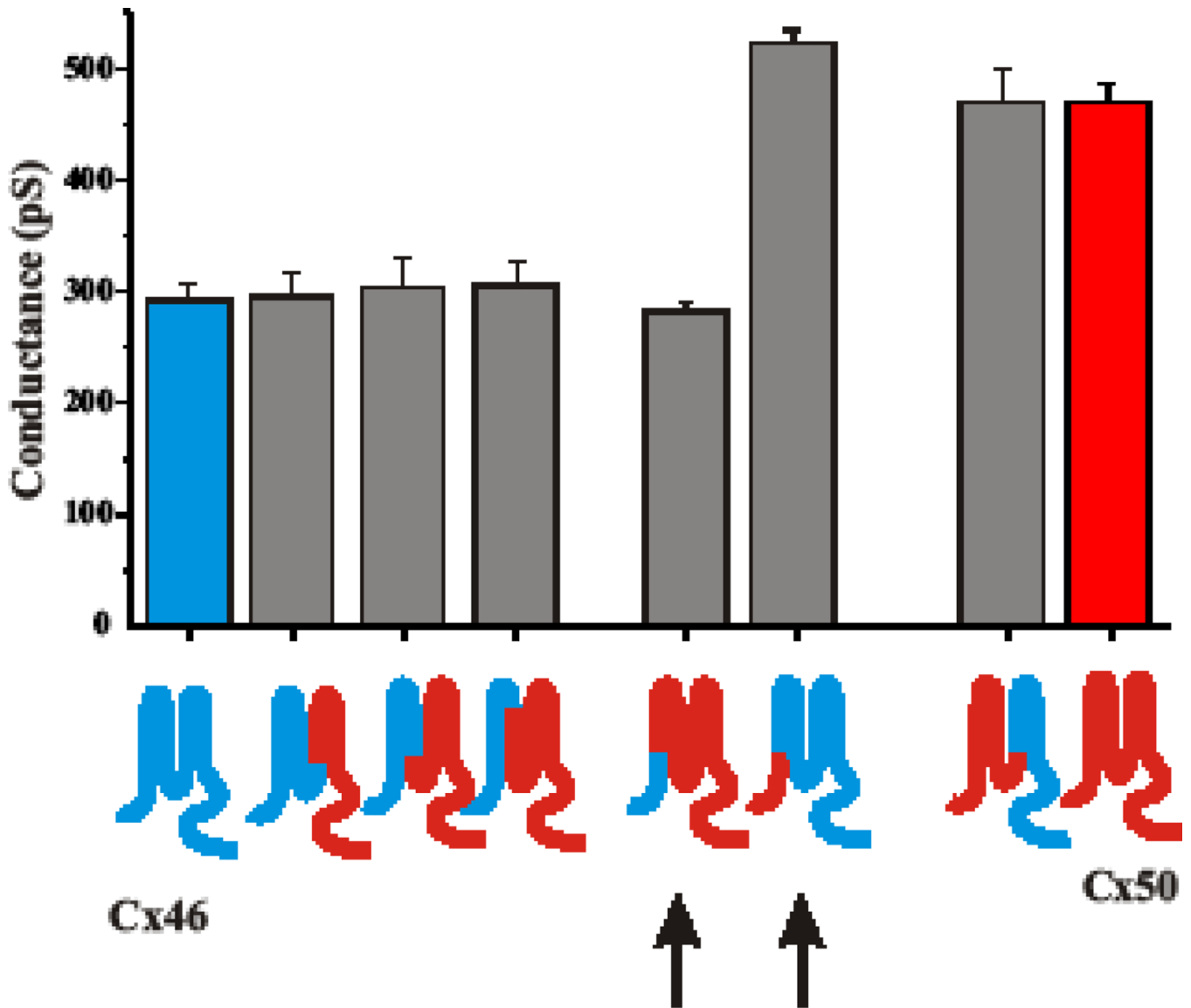
Fig. 5.
Unitary conductances of Cx46 and Cx50 hemichannels are specified by NT, E1 and TM1 domains. Shown is a bar graph summarizing unitary conductances of WT Cx46 (blue Cx) and WT Cx50 (red Cx). Unitary conductances represent slope conductances at $V_m = 0$ from fits to open channel I–V relations obtained by applying 8 sec ramps to patches containing single hemichannels. Sequence substituted in chimeras is indicated by color. Arrows denote substitutions of just NT domains.
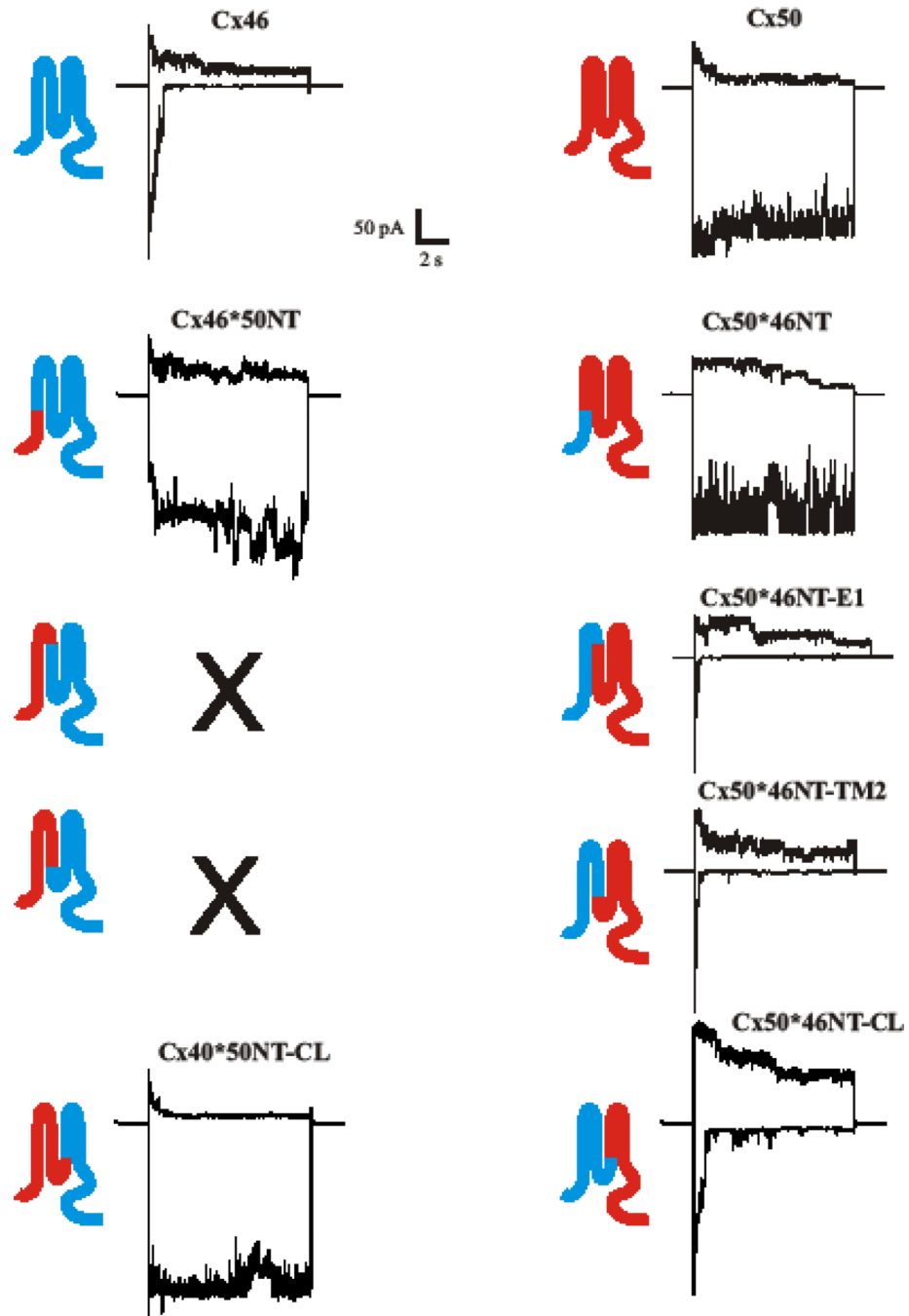
Fig. 6.
Gating of Cx46 and Cx50 hemichannels is specified by N-terminal half of the Cx protein, NT through CL. Shown are examples of currents obtained from patches containing multiple active hemichannels. Currents in response to positive (+40 mV) and negative (−90 mV) voltage steps are shown. WT Cx46 sequence is depicted in blue and WT Cx50 in red. Unitary conductances represent slope conductances at $V_m = 0$ from fits to open channel I–V relations obtained by applying 8 sec ramps to patches containing single hemichannels. Sequence substituted in the chimeras is indicated by color. Substitution of NT-E1 or NT-TM2 sequence of Cx50 onto Cx46 failed to form functional hemichannels.